

SPECIAL PROJECT PROGRESS REPORT

All the following mandatory information needs to be provided. The length should *reflect the complexity and duration* of the project.

Reporting year 2024

Project Title: Gravity Waves and Turbulence in the Free Atmosphere and the Atmospheric Boundary Layer

Computer Project Account: SPDESCAN

Principal Investigator: Dr. Andreas Dörnbrack

Affiliation: DLR Oberpfaffenhofen
Institut für Physik der Atmosphäre
Münchener Str. 20
D – 82230 WESSLING
Germany

Name of ECMWF scientist(s) collaborating to the project
(if applicable) Dr. Christian Kühnlein
Dr. Inna Polichtchouk
Dr. Nils Wedi
Dr. Peter Bechtold

Start date of the project: 2024

Expected end date: 2026

Computer resources allocated/used for the current year and the previous one (if applicable)

Please answer for all project resources

		Previous year		Current year	
		Allocated	Used	Allocated	Used
High Performance Computing Facility	(units)	500000	110000	500000	8000
Data storage capacity	(Gbytes)	80	80	80	80

Summary of project objectives (10 lines max)

This special project aims at combining high-resolution ground-based and airborne observations with IFS operational forecasts and analyses, with reanalyses, and with results from numerical modelling. The base of our measurements are airborne in-situ observations of the atmospheric wind and temperature in the upper troposphere and lower stratosphere as well as ground-based and airborne remote-sensing observations of temperature in the middle atmosphere. The goal is to analyse the properties of internal gravity waves and of turbulence in the stably stratified atmospheric airflow. A new aspect of our research will be the numerical simulation of the stably stratified atmospheric boundary layer where similar turbulent bursts are observed as in the free atmosphere. The challenge for numerical modelling is to achieve the needed high spatial and temporal resolutions. Furthermore, in this project we want to address the transition to modern computer architectures by applying the newly developed FVM of ECMWF to selected problems.

Summary of problems encountered (10 lines max)

No problems encountered

Summary of plans for the continuation of the project (10 lines max)

This project will be continued as planned.

List of publications/reports from the project with complete references

1. Dörnbrack, A., 2024: Transient Tropopause Waves, *Journal of the Atmospheric Sciences* under review.
2. Wrba, L., Englberger, A., Dörnbrack, A., Kilroy, G., and Wildmann, N., 2024: Data assimilation of realistic boundary-layer flows for wind-turbine applications – An LES study, *Wind Energ. Sci. Discuss.* [preprint], <https://doi.org/10.5194/wes-2024-12>, under review
3. Binder, M., & Dörnbrack, A., 2024: Observing gravity waves generated by moving sources with ground-based Rayleigh lidars. *Journal of Geophysical Research: Atmospheres*, 129, e2023JD040156. <https://doi.org/10.1029/2023JD040156>
4. Achatz, U., J. M. Alexander, E. Becker, H.-Y. Chun, A. Dörnbrack, L. Holt, R. Plougonven, I. Polichtchouk, K. Sato, A. Sheshadri, C. C. Stephan, A. van Niekerk, and C. J. Wright, 2024: Atmospheric Gravity Waves: Processes and Parameterization, *Journal of the Atmospheric Sciences*, **81**, 237–262, <https://doi.org/10.1175/JAS-D-23-0210.1>
5. Gupta, A., R. Reichert, A. Dörnbrack, H. Garny, R. Eichinger, I. Polichtchouk, B. Kaifler, and T. Birner, 2024: Estimates of Southern Hemispheric Gravity Wave Momentum Fluxes across Observations, Reanalyses, and Kilometer-Scale Numerical Weather Prediction Model. *J. Atmos. Sci.*, **81**, 583–604, <https://doi.org/10.1175/JAS-D-23-0095.1>.
6. Knobloch, S., B. Kaifler, A. Dörnbrack, and M. Rapp, 2023: Horizontal wavenumber spectra across the middle atmosphere from airborne lidar observations during a southern hemispheric SSW, *Geophysical Research Letters*, **50**, e2023GL104357. <https://doi.org/10.1029/2023GL104357>
7. Weimer, M., Wilka, C., Kinnison, D. E., Garcia, R. R., Bacmeister, J. T., Alexander, M. J., et al. (2023). A method for estimating global subgrid-scale orographic gravity-wave temperature perturbations in chemistry-climate models. *Journal of Advances in Modeling Earth Systems*, **15**, e2022MS003505. <https://doi.org/10.1029/2022MS003505>

Summary of selected results

(1) Observing Gravity Waves Generated by Moving Sources with Ground-Based Rayleigh Lidars (Binder and Dörnbrack, 2024)

Temperature measurements by zenith-pointing ground-based Rayleigh lidars are often used to detect middle atmospheric gravity waves, see as examples the plots in Figures 2 and 5. In time-height diagrams of observed or modelled temperature perturbations, stationary mountain waves are identifiable by horizontal phase lines. Vertically tilted phase lines, on the other hand, indicate that the wave source or the propagation conditions are transient. Idealized numerical simulations illustrate that and how a wave source moving in the direction of the mean wind entails upward-tilted phase lines, see Figure 1. The inclination angle depends on the horizontal wavelength and the propagation speed of the wave source.

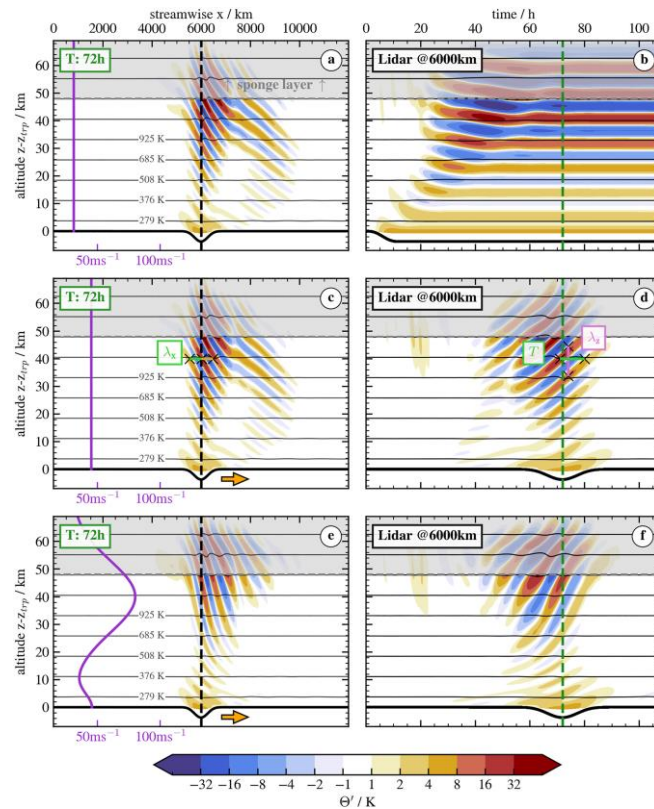


Figure 1: Vertical cross-sections (a), (c) and (e) after $t = 72$ h with ambient wind profiles in purple and time-height diagrams (b), (d) and (f) at the outlined position for three different simulations. The first simulation (a) and (b) features a stationary obstacle at the lower boundary and a constant wind profile. In the second simulation (c) and (d) the trough moves to the right with a constant speed $c_{tf} = 13.88 \text{ m s}^{-1}$ and the wind is increased by the same amount. The last simulation (e) and (f) represents a simulation with a more realistic stratospheric wintertime wind profile. The assessment of λ_z and period T from the time-height diagram is labeled in (d), two consecutive λ_x are labeled in (c). Contour lines represent constant potential temperature and the amplitude of the lower boundary is scaled by a factor of 5.

On this basis, the goal of the paper was to identify and characterize non-orographic gravity waves (NOGWs) from propagating sources, for example, upper-level jet/front systems, in simulated lidar observations and actual Rayleigh lidar measurements, see Figure 2. Composites of selected atmospheric variables from meteorological forecasts or reanalysis data are thoughtfully combined to associate NOGWs with processes in the troposphere and stratosphere, see Figure 3.

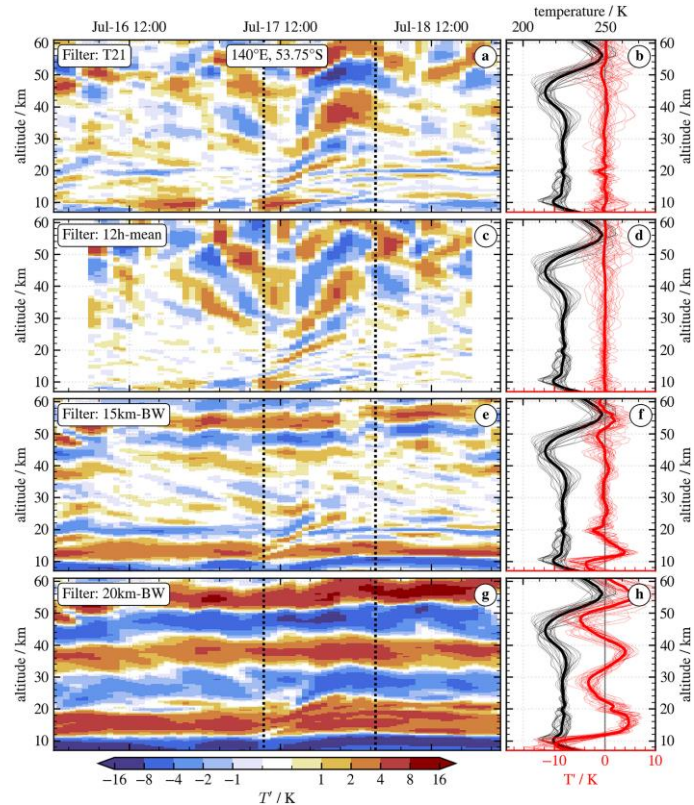


Figure 2: Time-height diagrams of stratospheric ERA5 T' for a location (140°E , 53.75°S) over the Southern Ocean (left column) and corresponding vertical profiles of absolute temperature and temperature perturbations (right column). Thick black and red lines in (b), (d), (f) and (h) are temporal mean profiles of absolute temperature and T' , respectively. Thin lines are individual profiles every 2 h. Panels (a) and (b) show temperature perturbations after subtracting the truncated temperature field T21 (horizontally filtered by removing wave numbers larger than 21) of the ERA5 dataset. Panels (c) and (d) show T' after removing a temporal running mean of 12 h. Panels (e) and (f) display the result of a vertical highpass Butterworth filter with a cutoff wavelength $\lambda_{cut} = 15$ km and panels (g) and (h) with $\lambda_{cut} = 20$ km.

The example also emphasizes that temporal filtering of temperature measurements is appropriate for NOGWs, especially in the presence of a strong polar night jet that implies large vertical wavelengths. During two selected observational periods of the Compact Rayleigh Autonomous Lidar (CORAL) in the lee of the southern Andes, upward-tilted phase lines are mainly associated with mountain waves and transient background wind conditions. One night-time measurement by CORAL coincides with the passage of an upper-level trough, but large-amplitude mountain waves superpose the small-amplitude NOGWs in the middle atmosphere.

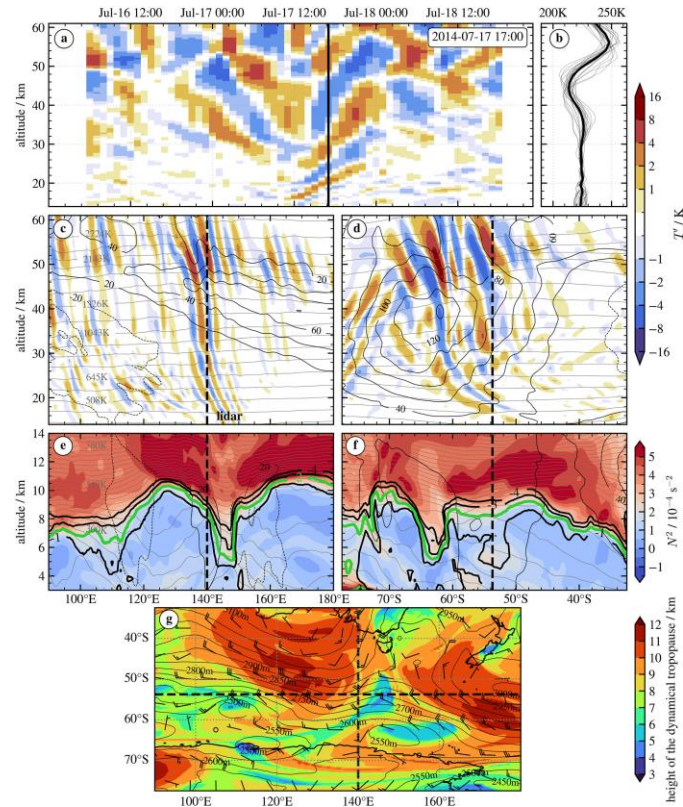


Figure 3: ERA5 overview for a location over the Southern Ocean (53.75°S, 140°E) during research flight RF25 of the DEEPWAVE campaign. Panels (a) and (b) are similar to Figures 2(c) and 2(d) emulating the measurements of a vertically staring ground-based lidar. Panels (c) and (d) are vertical sections of stratospheric T along sectors of the latitude circle (c) and meridian (d) of the virtual lidar location. (e) and (f) are corresponding vertical sections of thermal stability N^2 (10^{-4} s^{-2} , color-coded), potential temperature (K, thin gray lines), and potential vorticity (1, 2, 4 PVU: black, 2 PVU: green) in the vicinity of the dynamical tropopause. Thin black lines in the vertical sections are zonal (d) and (f) and meridional (c) and (e) wind components (solid: positive, dashed: negative). Panel (g) is a horizontal section of the height of the 2 PVU surface (km, color-coded), geopotential height (m, solid lines) and wind barbs at the 850 hPa level. The black vertical line in (a) marks the time (17 July 2014, 17 UTC) for (c)–(g) and dashed lines in (c)–(g) highlight the location of the virtual lidar and profiles in (a) and (b).

(2) Estimates of Southern Hemispheric Gravity Wave Momentum Fluxes across Observations, Reanalyses, and Kilometer-Scale Numerical Weather Prediction Model (Gupta et al., 2024)

Gravity waves are among the key drivers of the meridional overturning circulation in the mesosphere and upper stratosphere. Their representation in general circulation models suffers from insufficient resolution and limited observational constraints on their parameterizations. Both restrictions obscure assessments of middle atmospheric circulation changes in a changing climate. The study by Gupta et al. (2024) presents for a first time a comprehensive analysis of stratospheric gravity wave activity in an area above and downstream of the Andes from 1 to 15 August 2019, see Figure 4. Here, the special focus is on the representation of gravity waves ranging from an unprecedented kilometer-scale global forecast model (1.4 km ECMWF IFS, see Polichtchouk et al. 2023¹), ground-based Rayleigh lidar (CORAL) observations at Rio Grande, Argentina², modern reanalysis (ERA5), to a coarse-resolution climate model (EMAC), see Figures 5 and 6.

¹ Polichtchouk, I., A. van Niekerk, and N. Wedi, 2023: Resolved gravity waves in the extratropical stratosphere: Effect of horizontal resolution increase from $O(10)$ to $O(1)$ km. *J. Atmos. Sci.*, **80**, 473–486, <https://doi.org/10.1175/JAS-D-22-0138.1>.

² Kaifler, N., B. Kaifler, A. Dörnbrack, M. Rapp, J. L. Hormaechea, and A. de la Torre, 2020: Lidar observations of large-amplitude mountain waves in the stratosphere above Tierra del Fuego, Argentina. *Sci. Rep.*, **10**, 14529, <https://doi.org/10.1038/s41598-020-71443-7>.

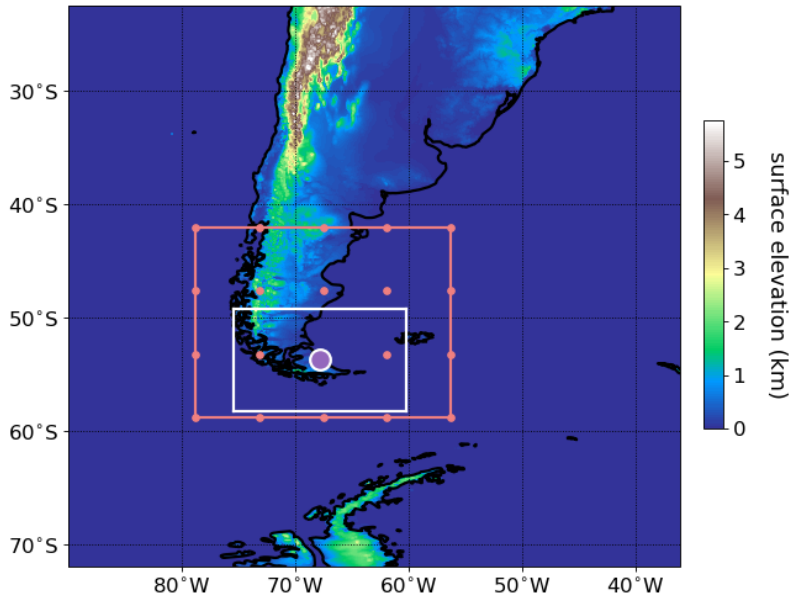


Figure 4: Variations in surface topography are shown in color using cylindrical projection. The violet dot shows the location of CORAL lidar at Rio Grande. The white box shows the 1000 km \times 1000 km box around Rio Grande used for two-dimensional wavelet analysis. The red grid box and dots shows the T21 grid used to conservatively interpolate high-resolution fluxes from IFS-1km and ERA5.

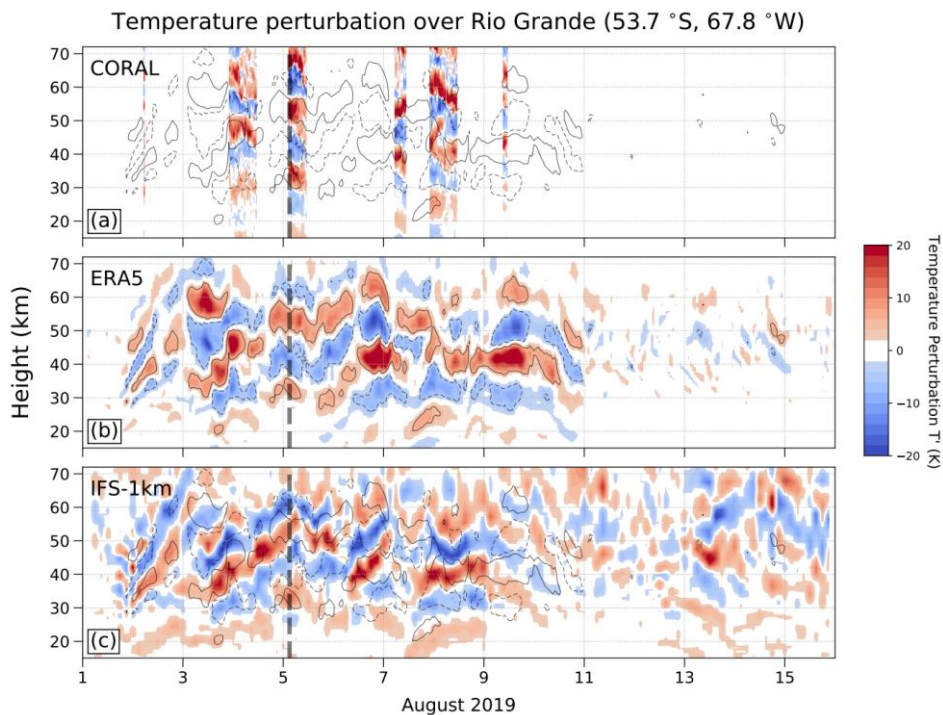


Figure 5: Vertical profiles of gravity wave-induced temperature perturbations (color) during 1-15 August 2019 over Rio Grande, Argentina (53.7 $^{\circ}$ S, 67.8 $^{\circ}$ W) from (a) ground-based Rayleigh lidar CORAL, (b) ERA5 reanalysis, and (c) ECMWF's IFS-1km free running model. The black curves in a-c show the ± 5 K temperature anomaly contours from ERA5, and are overlaid for reference. The dashed vertical bars in a-c mark the time 5 August 2019 03 UTC for which the horizontal profile of the GWs for ERA5 and IFS-1km are shown in Figure 6.

Resolved vertical flux of zonal gravity wave momentum (GWMF) is found to be stronger by a factor of at least 2–2.5 in IFS compared to ERA5. Compared to resolved GWMF in IFS, parameterizations in ERA5 and EMAC continue to inaccurately generate excessive GWMF poleward of 60 $^{\circ}$ S, yielding prominent differences between resolved and parameterized GWMFs. A like-to-like validation of GW profiles in IFS and ERA5 reveals similar

wave structures. Still, even at ~ 1 km resolution, the resolved waves in IFS are weaker than those observed by lidar.

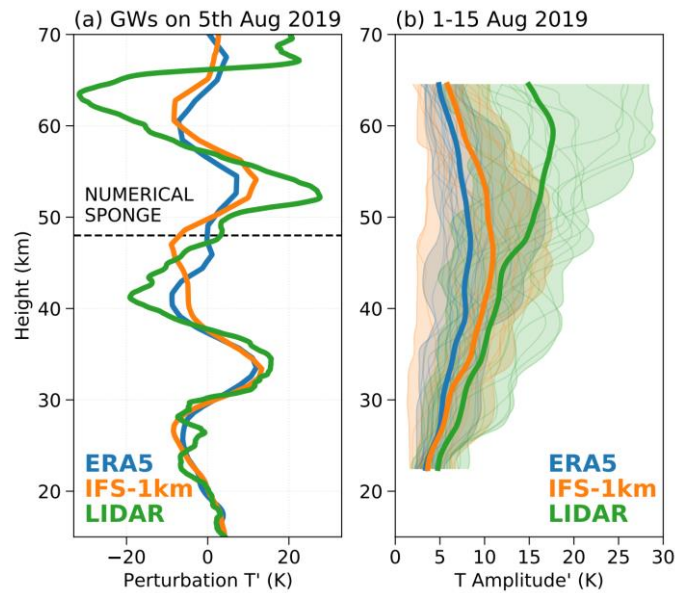


Figure 6: (a) Vertical profiles of temperature perturbations over Rio Grande in CORAL (green), IFS (orange), and ERA5 (blue), on 5 August 2019 03 UTC. The dashed black horizontal bar at 48 km marks the introduction of the mesospheric sponge. (b) Gravity wave amplitudes in the three models, obtained by vertically averaging the temperature magnitude over a centred 15-km vertical window. The bold curves show the time mean amplitude, while the individual thin curves enclosed within the respective shaded regions show the amplitudes at all the individual snapshots during 1-15 August 2019 for which the data is available.

Further, estimates of the gravity wave momentum fluxes across the datasets reveal that temperature-based proxies, based on mid-frequency approximations for linear gravity waves, overestimate its magnitude due to simplifications and uncertainties in estimates of the horizontal wavelength from data. Overall, the analysis provides GWMF benchmarks for parameterization validation and calls for three-dimensional gravity wave parameterizations, better upper-boundary treatment, and vertical resolution increases commensurate with increases in horizontal resolution in models, for a more realistic gravity wave analysis.